

# Study on the Application of Clustering Method in the Determination of Uncertainty Parameters of SWMM Model

**Chengshuai Liu**

Zhengzhou University

**Bingyan Ma**

Zhengzhou University

**Caihong Hu** (✉ [hucaihong@zzu.edu.cn](mailto:hucaihong@zzu.edu.cn))

Zhengzhou University

**Qiang Wu**

Zhengzhou University

**Yue Sun**

Zhengzhou University

**Xiang Li**

Zhengzhou University

---

## Research Article

**Keywords:** Urban flood simulation, SWMM, Parameter sample, Model uncertainty parameters, City functional area, K-means clustering algorithm

**Posted Date:** October 11th, 2021

**DOI:** <https://doi.org/10.21203/rs.3.rs-811017/v1>

**License:** © ⓘ This work is licensed under a Creative Commons Attribution 4.0 International License.

[Read Full License](#)

---

1                   **Study on the Application of Clustering Method in the Determination of**

2                                   **Uncertainty Parameters of SWMM Model**

3 Chengshuai Liu<sup>1</sup>, Bingyan Ma<sup>1</sup>, Caihong Hu<sup>1, ✉</sup>, Qiang Wu<sup>1</sup>, Yue Sun<sup>1</sup>, Xiang Li<sup>1</sup>

4           1 School of Water Conservancy Science and Engineering Zhengzhou University,  
5 Zhengzhou, 450001, China

6           ✉ Corresponding Author: Caihong Hu, School of Water Conservancy and  
7 Engineering, Zhengzhou University, 450001, China

8           Email address: hucaihong@zzu.edu.cn

9           **Abstract**

10           Storm Water Management Model (SWMM) is one of the most commonly used  
11 models in urban flood simulation. However, because the calibration and verification of  
12 the model's uncertainty parameters are extremely dependent on the measured flood data,  
13 it is difficult to apply the model in areas lacking data. This study proposes a parameter  
14 sample clustering method based on peer research results to determine the uncertainty  
15 parameters of SWMM, and compares the simulation results with the simulation results  
16 of the manual adjustment method based on measured data. The research shows that the  
17 Absolute error (*AE*), Relative error (*RE*), Nash efficiency coefficient (*NSE*), and  
18 Coefficient of determination ( $R^2$ ) of the water depth simulated by the parameter sample  
19 clustering method are 0.040m, 9.08%, 0.949, 0.967 compared with the measured value,  
20 respectively. The value of *AE*, *RE*, *NSE*, and  $R^2$  of the manual tuning method during the  
21 calibration simulation period are 0.066m, 15.95%, 0.881 and 0.924, respectively.  
22 Therefore, the parameter sample clustering method has a better simulation effect than

23 manual tuning method, and it can be further promoted in areas without flood data.

## 24 **Keywords**

25 Urban flood simulation; SWMM; Parameter sample; Model uncertainty parameters;  
26 City functional area; K-means clustering algorithm

## 27 **1 Introduction**

28 Urban flood disasters threaten the safety of people's lives and property and hinder  
29 the sustainable development of society and economy (Z. N. Wu et al. 2021; Xu et al.  
30 2020). Just in the past, the 7·20 rainstorm and waterlogging event in Zhengzhou City  
31 shocked the world. The extreme rainstorm caused 292 deaths in the city and the  
32 economic loss was as high as 65.5 billion yuan (Hu et al. 2021) . Accurate flood  
33 forecasting is an important non-engineering measure for flood prevention and disaster  
34 reduction (J. Y. Wang et al. 2020; Fu et al. 2020). In terms of non-engineering measures,  
35 through real-time high-precision urban rain and flood models or systems, accurate and  
36 effective early warning and forecasting of urban storm and flood processes have  
37 become the key to reducing disaster losses (Kastridis et al. 2020; Sarauskiene et al.  
38 2020). The measured precipitation-runoff data with high temporal and spatial  
39 resolution is the basis for reliable and accurate simulation and forecasting of urban rain  
40 and flood models (Luan et al. 2019). The number of existing urban hydrological  
41 stations, monitoring capabilities and station network density, especially the serious lack  
42 of real-time monitoring of urban pipeline flow, is far from meeting the needs of rain and  
43 flood warning and forecasting in the context of rapid urbanization (Fu et al. 2020).  
44 Because the calibration and verification problems in the modeling process of urban

45 storm flood model are directly related to the reliability of urban flood simulation  
46 (Hapuarachchi et al. 2011; Li et al. 2020). How to conduct rapid and efficient flood  
47 simulation in urban areas where data is lacking or without data has always been a  
48 research hot-spot in urban rain and flood simulation and forecasting (Luan et al. 2017).

49 In the application of urban flood simulation, the SWMM model is one of the most  
50 widely used representative models (Hu et al. 2020; Du, 2020). This study focuses on the  
51 parameter selection process of the SWMM model. SWMM model parameters are  
52 divided into deterministic parameters and uncertain parameters (de Souza et al. 2018;  
53 Liwanag et al. 2018). Among them, deterministic parameters have clear physical  
54 meanings. For example, the parameters of each sub-catchment include area,  
55 characteristic width, impermeability, slope, etc. (Liwanag et al. 2018); uncertainty  
56 Parameters such as depression storage volume in impervious area, depression storage  
57 volume in permeable area, impervious area Manning coefficient, permeable area  
58 Manning coefficient, etc (Mei, 2019). Uncertainty parameter model identification and  
59 verification of uncertainty parameters is the key content of SWMM model application  
60 (Mei et al. 2017).

61 In the actual application of the SWMM model, it is a recognized method to  
62 calibrate and verify model parameters based on a large number of measured flood  
63 events (Hu et al. 2020). However, this method needs to continuously adjust each  
64 sub-catchment according to the flood results, which is very time-consuming and  
65 complicated (Ma et al. 2020). In the absence of data, the method proposed by (Zaghloul,  
66 1983) to calibrate the parameters of the SWMM model based on the internal connection

67 and mutual influence between the runoff calculation parameters of the system  
68 analytical model and the spatial distribution of the catchment area (Zaghloul, 1983).  
69 Liu (2009) pointed out an urban rainfall runoff model verification method based on  
70 runoff coefficients was put forward under conditions; The model parameter calibration  
71 method combining surface runoff field observations and flood investigations has also  
72 been affirmed (Luan et al. 2017); With the help of physical processes and  
73 rainfall-runoff evolution mechanism research, Fu et al. (2020) obtained a verification  
74 method by generalizing the geometry of stagnant water. These methods are mainly used  
75 to deduce the model parameters through parameter transplantation, correlation analysis,  
76 empirical formulas, etc., and have achieved good results, but the complexity of manual  
77 parameter adjustment is still unavoidable. Nor can it take into account the differences in  
78 the value of the same parameter under the underlying conditions of complex cities.

79 For this reason, this study proposes a new method for the value of SWMM  
80 parameters. First, combining the land use type and the nature of land planning to divide  
81 the sub-catchment with the nature of a single urban functional area. Then use the  
82 K-means clustering method, a large number of peers' existing research results,  
83 combined with the principle of single city functional area value of the same parameter  
84 to assign parameters to the model, and finally compare and verify with the actual  
85 measured value. This can avoid the cumbersome and complicated adjustment of model  
86 parameters repeatedly, and at the same time provide a new model construction method  
87 for areas with no data.

## 88 **2 Methodology**

89 As shown in **Figure 1**, the focus of this research is based on the SWMM model,  
90 and the principle of parameter values for a single urban functional area is proposed.  
91 Based on this principle, a large number of peer research results parameters are selected  
92 as cluster calculation samples to obtain urban flood simulation calculations. The value  
93 of the model parameter. This method is called parameter sample clustering method, and  
94 compared with the traditional manual parameter adjustment method, it aims to improve  
95 the efficiency of model building and simulation accuracy.

### 96 **2.1 SWMM model**

97 The SWMM model was developed by the U.S. Environmental Agency in 1971  
98 and has been continuously improved (Xu et al. 2020). It is a widely used storm-water  
99 runoff simulation software (Gironas et al. 2010). It is widely used to simulate a single  
100 precipitation event in a city or long-term water volume, water quality simulation and  
101 sponge city research (X. Wu et al. 2017; Xiang et al. 2017; Zhang et al. 2017).

102 The SWMM model has the advantages of simple operation, short calculation time,  
103 and relatively reliable calculation results (van der Sterren et al. 2014), but it has  
104 disadvantages such as rough division of sub-catchments and complex parameter  
105 adjustment (Z. N. Wu et al. 2020). In particular, the calibration and verification of its  
106 uncertainty parameters need to rely on measured flood data (Hu et al. 2020), which  
107 makes it difficult for SWMM to be applied in urban areas without data.

108 SWMM parameters can be divided into deterministic parameters and uncertain  
109 parameters (As shown in **Table 1**). The deterministic parameters include eight

110 parameters: Sub-catchment area (SA), Characteristic width (CW), Impervious area rate  
111 (IAR), Slope (SL), Node elevation (NE), Pipeline shape (PS), Pipeline length (PL), and  
112 Pipeline inner bottom elevation (PBE). These parameters can be obtained by field  
113 measurement or software analysis. The uncertainty parameters of the SWMM model  
114 mainly include the Impervious area depression (DI), Impervious area Manning  
115 coefficient (NI), Permeable area depression (DP), Permeable area Manning coefficient  
116 (NP), Maximum infiltration rate (MAX), Minimum infiltration rate (MIN), Attenuation  
117 coefficient (DE) and Pipeline Manning Ning coefficient (MC) 8 parameters (Du. 2020).

118 The sensitivity of model uncertainty parameters is related to factors such as  
119 rainfall characteristics and underlying surface conditions (Gironas et al. 2010; Xu et al.  
120 2020). Different studies have different values of DI, NI, DP, and NP. The surface  
121 depression storage volume reflects the depression storage depth of the hydrological  
122 response unit, and the surface Manning coefficient reflects the resistance of  
123 precipitation when it passes through the hydrological response unit (X. Wu et al. 2017;  
124 Xiang et al. 2017). Under the conditions of low slope and small topography in plain  
125 cities, surface depression storage and surface Manning coefficient become more  
126 significant sensitive parameters, and their correlation with urban surface characteristics  
127 is relatively large. Therefore, we select four uncertainty parameters DI, NI, DP, and NP  
128 for sample clustering (Li. 2016).

## 129 **2.2 Divide the sub-catchment**

130 The division of sub-catchments is one of the main steps of SWMM model  
131 modeling, and the quality of the division has a relatively large impact on the accuracy of

132 the results (Chen et al. 2018; de Souza et al. 2018; Gironas et al. 2010; Xu et al. 2020).  
133 We refer to previous research and refine the following division steps : 1) The surface of  
134 the city has both natural and social attributes, and the two attributes are superimposed to  
135 divide the city's functions ; 2) Analyze the topography and confluence characteristics  
136 of the study area, determine the drainage area, and use the distribution of the drainage  
137 network trunk pipes and trunk roads as the division skeleton ; 3) Control the number  
138 and spatial scale, and the ratio of the number of pipe sections and nodes to the number  
139 of sub-catchments is mostly 0.6-1.4 ; 4) Divide the sub-catchment area so that there is  
140 only one urban functional area in the hydrological response unit.

### 141 **2.3 SWMM model parameter clustering calculation**

142 The K-means clustering algorithm in the statistical analysis method is used to  
143 calculate the model parameters. It is an iterative solution clustering analysis algorithm  
144 (C. Wang et al. 2021). It often selects  $K$  objects randomly as the initial cluster centers,  
145 and then calculates the various sub-clusters of each object distance The distance  
146 between centers assigns each object to the cluster center closest to it (Liu et al.2015;  
147 Qian et al.2012).

148 In the process of clustering, determining the number of classes is a common  
149 problem faced by all clustering methods. The K-Means clustering analysis method  
150 selects the optimal number of classifications through analysis of variance, that is,  
151 defines an F statistic:



$$F = [S_{SA} / (k - 1)] / [S_{SE} / (n - k)]$$

152

$$S_{SA} = \sum_{i=1}^k n_i (x_i - \bar{x}_i)^2$$

$$S_{SE} = \sum_{i=1}^k \sum_{j=1}^{n_i} (x_{ij} - \bar{x}_i)^2$$

153

In the formula,  $k$  is the number of clusters,  $n_i$  is the sample size of the  $i$ -th

154

class,  $S_{SA}$  is the sum of squared deviations between groups,  $S_{SE}$  is the sum of squared

155

deviations within the group,  $n$  is the total number of samples, and  $x_i$  is the size of the

156

$i$ -th class. The sample value,  $\bar{x}_i$  represents the sample average of the  $i$ -th class, and

157

$x_{ij}$  represents the observation value of the  $j$ -th index of the  $i$ -th class.

158

According to the research purpose, the appropriate clustering index is selected,

159

and the sample data is standardized to eliminate the difference in dimensions. There are

160

$m$  sample groups, and each sample group has  $P$  index data. These  $m \times P$  data

161

constitute a parameter clustering observation matrix, namely:

162

$$x = \begin{bmatrix} x_{11} & x_{12} & \dots & x_{1p} \\ x_{21} & x_{22} & \dots & x_{2p} \\ & & \dots & \\ & & \dots & \\ & & \dots & \\ x_{m1} & x_{m2} & \dots & x_{mp} \end{bmatrix}$$

163

Among them,  $x_{i'j'}$  is the  $j'$ -th index parameter value of the  $i'$ -th sample group,  $i'$

164

$= 1, 2, \dots, m$ ,  $j' = 1, 2, \dots, p$ ; then:

$$\bar{x}_{j'} = \frac{1}{m} \sum_{i=1}^m x_{ij'}$$

165

$$s_{j'} = \left[ \frac{1}{m-1} \sum_{i=1}^m (x_{ij'} - \bar{x}_{j'})^2 \right]^{1/2}$$

$$y_{ij'} = (x_{ij'} - \bar{x}_{j'}) / s_{j'}$$

166 In the formula,  $\bar{x}_j$  is the mean value of the  $j$ 'th index parameter;  $s_j$  is the  
167 standard deviation of the  $j$ 'th index parameter;  $y_{ij}$  is the standardized value of the  
168 parameter value  $x_{ij}$ .

#### 169 **2.4 Model evaluation Indicator Selection**

170 The absolute error ( $AE$ ) is the absolute value of the difference between the  
171 measured value and the true value. Here it refers to the absolute value of the difference  
172 between the simulated water depth of the model and the actual measured water depth  
173 (Hu et al. 2018). The mathematical expression is as follows:

$$174 \quad AE = |S_i - O_i|$$

175 where  $S_i$  and  $O_i$  are the simulated and observed water depth at the  $i$ -th number.

176 Relative error ( $RE$ ) refers to the value obtained by multiplying the ratio of the  
177 absolute error caused by the measurement to the measured (conventional) true value by  
178 100%, expressed as a percentage. Generally speaking, the relative error can better  
179 reflect the credibility of the measurement. It is mostly used in the evaluation of urban  
180 rain and flood models to indicate the credibility of the simulated value of flood peak  
181 discharge (Hu et al. 2018). It is described as follows:

$$182 \quad RE = \frac{S_i - O_i}{O_i} \times 100\%$$

183 where  $S_i$  and  $O_i$  are the simulated and observed water depth at the  $i$ -th number.

184 The mathematical expressions of these metrics can be described as follows (J.E. et  
185 al. 1970):

186

$$NSE = 1 - \frac{\sum_{i=1}^n (S_i - O_i)^2}{\sum_{i=1}^n (S_i - \bar{O})^2}$$

187

where  $S_0$  (m) and  $O_0$  ( $m^3/s$ ) represent the water depth of the simulated and

188

observed hydrographs, respectively;  $\bar{O}$  is the mean value of the observed water depth,

189

and  $n$  is the data points number.  $NSE$  measures the ability of the model to predict

190

variables different from the mean, gives the proportion of the initial variance accounted

191

for by the model, and ranges from 1 (perfect fit) to  $-\infty$ . Values closer to 1 provide more

192

accurate predictions (Gupta et al. 1999).

193

The coefficient of determination ( $R^2$ ) is often used to describe the degree of fit

194

between data (Hu et al. 2018). When  $R^2$  is closer to 1, it means that the reference value

195

of the related equation is higher; on the contrary, when it is closer to 0, it means that the

196

reference value is lower. It is described as follows:

197

$$R^2 = \frac{\left[ \sum_{i=1}^n (S_i - \bar{S})(O_i - \bar{O}) \right]}{\sum_{i=1}^n (S_i - \bar{S})^2 (O_i - \bar{O})^2}$$

198

where  $n$  is the total number of measured data,  $S_i$  is the simulated water depth for

199

data point  $i$ ,  $O_i$  is the measured water depth for data point  $i$ , and is the averaged value of

200

the measured water depth (Jackson et al. 2019).

201

### **3 Results and discussion**

202

#### **3.1 Study area**

203

The geographical coordinates of Zhengzhou City are  $112^{\circ}42'$ - $114^{\circ}14'$  E and

204

$34^{\circ}16'$ - $34^{\circ}58'$  N. It belongs to the continental monsoon climate in the northern

205

temperate zone, with hot and rainy summers and autumns, cold and dry springs and

206 winters, with an average annual rainfall of 542 mm. The basic terrain tends to be low in  
207 the northwest and high in the southeast, with serious waterlogging during the flood  
208 season (J. Y. Wang et al. 2020). Zhengzhou University is located in the West Fourth  
209 Ring of Zhengzhou City. The climate characteristics of the school are consistent with  
210 those of Zhengzhou City. On the whole, the building pattern and drainage pipe network  
211 of Zhengzhou University are distributed in a gridded rectangle, which is very beneficial  
212 to the division of the sub-catchment of the model, as shown in **Figure 2**.

### 213 **3.2 Database**

214 According to research needs, we collected rainfall data from Henan Hydrological  
215 Bureau during 2014-2018; and obtained the water depth of the outlet node of  
216 Zhengzhou University through experimental monitoring. The land use data is visually  
217 interpreted by Google's high-definition image map and corrected on-site, with an  
218 accuracy of 1×1m. The pipe network data comes from the Infrastructure Management  
219 Office of Zhengzhou University. The elevation data is obtained through surveying and  
220 mapping. Uncertain parameter samples are derived from 26 research results published  
221 by peers.

222 **Table 2** shows the rainfall information of 6 flood events. Corresponding to the  
223 rainfall data, we selected 6 flood events to calibrate the parameters of the model to  
224 compare the reliability of the manual tuning method and the parameter sample  
225 clustering method.

226 **Table 3** is the sample data used to calculate the clustering parameters. There are 26  
227 research results published by peers in total. Because this research is aimed at the

228 application of the SWMM model in China, the previous results of the selected peers are  
229 all in the research area of China.

### 230 **3.3 Sub-catchment area division**

231 According to the requirements of China's current "Outdoor Drainage Design  
232 Code", the pipeline network is generalized. The pipeline network is generalized into  
233 node elevation, pipeline shape, length, pipe diameter, etc., and combined with pipeline  
234 network distribution information, topography, and surface type information, the study  
235 area Divided into 29 sub-catchments, 37 nodes, 37 pipes and 1 total water outlet, of  
236 which the pipes and water outlets are free flow. Considering factors such as actual  
237 topography, land use type, and location of drainage pipe network to divide  
238 sub-catchment areas. Ensure that each sub-catchment is an independent urban  
239 functional area. As shown in **Figure 3**.

240 The division of land use types is an important prerequisite for the division of  
241 sub-catchments. The land use type of the study area is determined by visual  
242 interpretation of the 1×1m high-definition remote sensing method, and field inspections  
243 are used to make corrections, so as to ensure the division of sub-catchments. Reliability  
244 of the natural attributes of the water area. On the whole, Zhengzhou University's  
245 architectural pattern and drainage pipe network are grid-shaped and rectangular. The  
246 drainage pipe network is relatively independent and systematic. This is very beneficial  
247 to the model's sub-catchment division, which ensures the society of sub-catchment  
248 divisions. Attribute reliability.

### 249 **3.4 Parameter clustering results**

250 The urban surface has both natural and social attributes, and the two attributes are  
251 superimposed to divide the city's functions (Du, 2020). It is divided into three types:  
252 industrial and commercial areas (ICA), residential areas (RA), and public areas (PA).

253 Taking the values of these parameters in **Table 3** as samples, the K-means  
254 clustering algorithm is used to calculate the parameter values on different urban  
255 functional areas, the number of clusters  $K$  is set to 3. This also refers to the number of  
256 functional districts in the city and the parameters clustering results are shown in **Table**  
257 **4**.

258 For other parameters, the calculation results of flood control and drainage in  
259 Zhengzhou City (Li et al., 2016) are used as the values of model parameters. Among  
260 them, MAX is 76.2mm/h; MIN is 3.6mm/h; DE is 3; MC is 0.014.

261 The cluster classification results of DI, NI, DP, and NP are shown in **Figure 4**. The  
262 three axes are composed of parameter values, sample size, and fixed width. The fixed  
263 width has no practical meaning. The light gray separation layer represents the dividing  
264 line of the sample parameter clustering, and the category number corresponding to the  
265 Roman numeral. The black arrows represent the cluster centers of each category. These  
266 four parameters are divided into three ranges, and the different categories are caused by  
267 the differences in the underlying surface conditions. The industrial and commercial  
268 area in the study area is mainly used for commercial and financial land. It is located in  
269 the center of the study area with convenient traffic and on both sides of the main traffic  
270 line (street) or at the corner intersection. The buildings are tall and dense, and the

271 hardened road surface is flat and densely distributed. The depression has the smallest  
272 storage capacity and the smallest surface Manning coefficient; residential areas are  
273 located outside or around the industrial and commercial districts, residential areas are  
274 fragmented, high- and low-differentiated, public facilities are complete, the layout is  
275 complete, and the environmental quality is good. At the same time, its building density  
276 and floor area ratio are controlled. It has both hardened roads and roofs, as well as a  
277 green area rate of about 30%. The surface depressions are moderately stocked and the  
278 surface Manning coefficient is moderate; the public areas are mainly comprehensive  
279 parks and specialized parks, with certain recreational facilities and service facilities.  
280 The green land, which has the comprehensive functions of improving the ecology,  
281 beautifying the city, and preventing and reducing disasters, has certain permeability and  
282 water storage capacity. Therefore, in the sub-catchment area, the surface depression has  
283 the largest storage capacity and the surface Manning coefficient is the largest.

### 284 **3.5 Model parameter evaluation**

285 The focus of this research is to compare the application effects of manual  
286 adjustment method and parameter sample clustering method in SWMM model for  
287 flood simulation. The difference is that the manual tuning method consists of two parts:  
288 parameter calibration and verification, while the parameter sample clustering method  
289 only has parameter clustering. Therefore, we selected 6 flood events of 20140524,  
290 20150707, 20160605, 20170812, 20180801, 20180818 to compare the simulation  
291 results. Among them, in the manual debugging method, the three flood events of  
292 20140524, 20150707, and 20160605 were used for calibration, and the three flood

293 events of 20170812, 20180801, and 20180818 were used for verification.

294 As shown in **Figure 5**. Orange represents Precipitation, and the black square  
295 dotted line represents the measured water depth change process. The blue circular  
296 dotted line represents the simulation result of the manual tuning method, and the red  
297 triangle represents the simulation result of the parameter sample clustering method. As  
298 a whole, it seems that the parameter sample clustering method is closer to the measured  
299 process line.

300 Although it is difficult to simulate the water depth change process at the outlet of  
301 the urban drainage network, the parameter sample clustering method and manual  
302 adjustment method both show good simulation results (as shown in **Figure 5**). In the  
303 simulation of the peak water depth period, the parameter sample clustering method is  
304 closer to the measured value than the manual adjustment method, but both are smaller  
305 than the measured value. In the retreat stage, the same parameter sample clustering  
306 method is closer to the measured value than the manual adjustment method, but both  
307 are larger than the measured value. Therefore, the parameter sample clustering method  
308 has a better simulation effect than the manual tuning method.

309

310 The above research is a qualitative macro-analysis. **Table 5** quantitatively  
311 compares the prediction performance of runoff depth of the SWMM model using  
312 manual adjustment method and parameter sample clustering method. Four performance  
313 indicators of  $AE$ ,  $RE$ ,  $NSE$  and  $R^2$  were used to evaluate them respectively. When the  
314 manual adjustment method is used, the  $AE$  and  $RE$  of the simulation results of the water



315 depth change process during the calibration period are both less than 0.07m, 15%, and  
316 the *NSE* is greater than 0.880; the *AE* and *RE* of the simulation results during the  
317 verification period are both less than 0.09m, 20%, and the *NSE* is greater than 0.850.  
318 This shows that the traditional model parameter debugging can still guarantee the  
319 simulation accuracy of the SWMM model. When using the parameter sample clustering  
320 method, the *AE* and *RE* of the simulation results of the water depth change process  
321 during the calibration period are both less than 0.06m, 12%, and the *NSE* are both  
322 greater than 0.910; the *AE* and *RE* of the simulation results during the verification  
323 period are both less than 0.06m, 11%, and the *NSE* is both Greater than 0.950. This  
324 shows that the parameter sample clustering method can significantly improve the  
325 simulation accuracy of the SWMM model. This conclusion can be better reflected in  
326 the difference between the performance evaluation indicators of the two methods. In the  
327 6 flood events, when the SWMM model uses the sample parameter clustering method,  
328 the *AE* and *RE* are both decreasing, and the *NSE* is increasing.

329 **Figure 6** is the correlation diagram of the simulated water depth change process  
330 and actual measured value of the SWMM model using two simulation methods. The  
331 abscissa is the actual measured value, and the ordinate is the simulated value. **Figure**  
332 **6(a)** is the manual adjustment method. We can see that the water depth data The points  
333 are clustered near the 45° line, and the  $R^2$  value is 0.924, but there are still some water  
334 depth data points showing scattered characteristics; **Figure 6(b)** is the simulation result  
335 of the parameter sample clustering method, and we can see that the water depth data  
336 points are more concentrated Is concentrated near the 45° line, and the  $R^2$  value is 0.967,

337 which shows that the SWMM model has higher simulation accuracy when using the  
338 parameter sample clustering method to determine the model parameters.

339 We propose to improve the parameter value of the SWMM model based on the  
340 parameter value principle of a single city functional area. The research results show that  
341 the parameters determined by the sample parameter clustering method have higher  
342 accuracy when the SWMM model simulates urban flooding. In the process of using the  
343 SWMM model, the traditional manual parameter adjustment method takes a long time  
344 and cannot avoid the phenomenon of "different parameters with the same effect", which  
345 has obvious shortcomings. Of course, this does not mean that the manual tuning method  
346 is completely inapplicable. On the contrary, the parameter sample clustering method  
347 proposed in this study is essentially to obtain samples from a large number of  
348 peer-to-peer tuning results. Mining the data clustering characteristics of the same  
349 parameter, and interpreting this characteristic as the difference of urban functional areas,  
350 so as to better ensure the simulation ability and efficiency of the SWMM model. The  
351 research results can also be used in urban areas where there is no measured  
352 rainfall-runoff data.

#### 353 **4 Conclusion**

354 This paper applies the SWMM model to urban flood simulation, and proposes a  
355 calculation method based on the clustering of parameter samples of a single city  
356 functional area, and the following conclusions are obtained:

357 1. The SWMM model has a good rainfall-flood simulation effect in urban areas.  
358 Through manual adjustment of parameters, during the application process, the average

359 values of *AE*, *RE* and *NSE* during the calibration period are 0.051m, 12.93%, and 0.888  
360 respectively; the average of the verification period The average values of *AE*, *RE*, and  
361 *NSE* are 0.066m, 15.95%, and 0.881, respectively. Using the improved SWMM model  
362 using the parameter sample clustering method, the average values of *AE*, *RE*, and *NSE*  
363 are 0.040m, 9.08%, and 0.949, respectively; the various evaluation indicators are better  
364 than the manual adjustment method.

365 2. Using parameter sample clustering method to calculate the SWMM model  
366 parameters is more applicable than manual tuning method. Compared with the  
367 measured value, the  $R^2$  value of the former is 0.959, and the  $R^2$  value of the latter is  
368 0.924. It shows that this method can replace the traditional manual parameter  
369 adjustment method, and can further carry out flood simulation in urban areas without  
370 data. In the process of constructing and using SWMM, the sample parameter clustering  
371 method is more efficient than the manual parameter adjustment method, which greatly  
372 simplifies the parameter selection process of SWMM. This is of great significance to  
373 the promotion and application of the model.

374 3. After calculating the same parameters through sample clustering, the values of  
375 the cluster centers are different. This difference may be caused by the difference in the  
376 underlying surface conditions. Among them, PA (road, hard block) has the largest DI,  
377 DP, NI, and NP; RA (residential area) has the second highest DI, DP, NI, and NP; ICA  
378 has the smallest DI, DP, NI, and NP. Therefore, if SWMM takes different parameter  
379 values in different urban functional zones, the model can reflect the spatial variation  
380 characteristics of the urban surface.

381 **Authors Contributions**

382 For this research paper with several authors, a short paragraph specifying their  
383 individual contributions was provided. Chengshuai Liu developed the original idea and  
384 contributed to the research design for the study. Bingyan Ma was responsible for data  
385 collecting. Caihong Hu provided guidance and contributed to the research design.  
386 Qiang Wu, Yue Sun, and Xiang Li provided some guidance for the writing of the article.  
387 All authors have read and approved the final manuscript.

388 **Funding**

389 This work was funded by Key projects of National Natural Science Foundation of  
390 China, grant number 51739009, National Natural Science Foundation of China, grant  
391 number 51979250.

392 **Declaration of competing interest**

393 The authors declare that there is no conflict of interest regarding the publication of  
394 this paper.

395 **Availability of data and material**

396 Not applicable. The data in this manuscript is also used in other ongoing research,  
397 so data and materials are not applicable.

398 **References**

399 Chen, W. J., Huang, G. R., Zhang, H., & Wang, W. Q. (2018). Urban inundation  
400 response to rainstorm patterns with a coupled hydrodynamic model: A case  
401 study in Haidian Island, China. *Journal of Hydrology*, 564, 1022-1035.  
402 Retrieved from <Go to ISI>://WOS:000445316200080.

403 doi:10.1016/j.jhydrol.2018.07.069

404 Du Xian. Research on the refined simulation of urban rainstorm and flood based on  
405 SWMM model [D]. Zhengzhou University, 2020.

406 de Souza, B. A., Paz, I. d. S. R., Ichiba, A., Willinger, B., Gires, A., Amorim, J. C.  
407 C., . . . Schertzer, D. (2018). Multi-hydro hydrological modelling of a complex  
408 peri-urban catchment with storage basins comparing C-band and X-band radar  
409 rainfall data. *Hydrological Sciences Journal-Journal Des Sciences*  
410 *Hydrologiques*, 63(11), 1619-1635. Retrieved from <Go to  
411 ISI>://WOS:000450274900003. doi:10.1080/02626667.2018.1520390

412 Gironas, J., Roesner, L. A., Rossman, L. A., & Davis, J. (2010). A new applications  
413 manual for the Storm Water Management Model (SWMM). *Environmental*  
414 *Modelling & Software*, 25(6), 813-814. Retrieved from <Go to  
415 ISI>://WOS:000276030300014. doi:10.1016/j.envsoft.2009.11.009

416 Gupta, H. V., Sorooshian, S., & Yapo, P. O. (1999). Status of Automatic Calibration  
417 for Hydrologic Models: Comparison with Multilevel Expert Calibration.  
418 *Journal of Hydrologic Engineering*, 4(2).

419 Hapuarachchi, H. A. P., Wang, Q. J., & Pagano, T. C. (2011). A review of advances in  
420 flash flood forecasting. *Hydrological Processes*, 25(18), 2771-2784. Retrieved  
421 from <Go to ISI>://WOS:000294201200001. doi:10.1002/hyp.8040

422 Hu, C. H., Liu, C. S., Yao, Y. C., Wu, Q., Ma, B. Y., & Jian, S. Q. (2020). Evaluation  
423 of the Impact of Rainfall Inputs on Urban Rainfall Models: A Systematic  
424 Review. *Water*, 12(9). Retrieved from <Go to ISI>://WOS:000580334000001.

425 doi:10.3390/w12092484

426 Hu, C. H., Wu, Q., Li, H., Jian, S. Q., Li, N., & Lou, Z. Z. (2018). Deep Learning with  
427 a Long Short-Term Memory Networks Approach for Rainfall-Runoff  
428 Simulation. *Water*, *10*(11), 16. Retrieved from <Go to  
429 ISI>://WOS:000451736300050. doi:10.3390/w10111543

430 Hu Yuwei, Li Hao, Hao Shuangyan, Aoki, Chen Kang, Liu Yupeng. The world pays  
431 attention to China's rainstorm rescue [N]. *Global Times*, 2021-07-23 (016).

432 J.E., N., & J.V., S. (1970). River flow forecasting through conceptual models part I: A  
433 discussion of principles. *Elsevier*, *10*(3).

434 Jackson, E. K., Roberts, W., Nelsen, B., Williams, G. P., Nelson, E. J., & Ames, D. P.  
435 (2019). Introductory overview: Error metrics for hydrologic modelling - A  
436 review of common practices and an open source library to facilitate use and  
437 adoption. *Environmental Modelling & Software*, *119*, 32-48. Retrieved from  
438 <Go to ISI>://WOS:000478965700003. doi:10.1016/j.envsoft.2019.05.001

439 Kastridis, A., Kirkenidis, C., & Sapountzis, M. (2020). An integrated approach of  
440 flash flood analysis in ungauged Mediterranean watersheds using post-flood  
441 surveys and unmanned aerial vehicles. *Hydrological Processes*, *34*(25),  
442 4920-4939. Retrieved from <Go to ISI>://WOS:000575128500001.  
443 doi:10.1002/hyp.13913

444 Li Shihao. Flood Risk Analysis and Waterlogging Simulation Research in Zhengzhou  
445 City[D]. Zhengzhou University, 2016.

446 Li, Q., Liang, Q. H., & Xia, X. L. (2020). A novel 1D-2D coupled model for

447 hydrodynamic simulation of flows in drainage networks. *Advances in Water*  
448 *Resources*, 137, 14. Retrieved from <Go to ISI>://WOS:000519527900013.  
449 doi:10.1016/j.advwatres.2020.103519

450 Liwanag, F., Mostrales, D. S., Ignacio, M. T. T., & Orejudos, J. N. (2018). Flood  
451 Modeling Using GIS and PCSWMM. *Engineering Journal-Thailand*, 22(3),  
452 279-289. Retrieved from <Go to ISI>://WOS:000437090700021.  
453 doi:10.4186/ej.2018.22.3.279

454 Luan, Q. H., Fu, X. R., Song, C. P., Wang, H. C., Liu, J. H., & Wang, Y. (2017).  
455 Runoff Effect Evaluation of LID through SWMM in Typical Mountainous,  
456 Low-Lying Urban Areas: A Case Study in China. *Water*, 9(6), 21. Retrieved  
457 from <Go to ISI>://WOS:000404559900077. doi:10.3390/w9060439

458 Ma, B. Y., Wu, Z. N., Wang, H. L., & Guo, Y. (2020). Study on the Classification of  
459 Urban Waterlogging Rainstorms and Rainfall Thresholds in Cities Lacking  
460 Actual Data. *Water*, 12(12). Retrieved from <Go to  
461 ISI>://WOS:000602841700001. doi:10.3390/w12123328

462 Sarauskiene, D., Akstinas, V., Nazarenko, S., Kriauciuniene, J., & Jurgelenaite, A.  
463 (2020). Impact of physico-geographical factors and climate variability on flow  
464 intermittency in the rivers of water surplus zone. *Hydrological Processes*,  
465 34(24), 4727-4739. Retrieved from <Go to ISI>://WOS:000574046800001.  
466 doi:10.1002/hyp.13912

467 van der Sterren, M., Rahman, A., & Ryan, G. (2014). Modeling of a lot scale  
468 rainwater tank system in XP-SWMM: A case study in Western Sydney,

469 Australia. *Journal of Environmental Management*, 141, 177-189. Retrieved  
470 from <Go to ISI>://WOS:000338599800020.  
471 doi:10.1016/j.jenvman.2014.02.013

472 Wang, C., & Wu, D. H. (2021). A K-Means Clustering-Based Multiple Importance  
473 Sampling Algorithm for Integral Global Optimization. *Journal of the*  
474 *Operations Research Society of China*(prepublish).

475 Wang, J. Y., Hu, C. H., Ma, B. Y., & Mu, X. L. (2020). Rapid Urbanization Impact on  
476 the Hydrological Processes in Zhengzhou, China. *Water*, 12(7). Retrieved from  
477 <Go to ISI>://WOS:000558701300001. doi:10.3390/w12071870

478 Wu, X., Wang, Z., Guo, S., Liao, W., Zeng, Z., & Chen, X. (2017). Scenario-based  
479 projections of future urban inundation within a coupled hydrodynamic model  
480 framework: A case study in Dongguan City, China. *Journal of Hydrology*, 547,  
481 428-442. Retrieved from <Go to ISI>://WOS:000398871100032.  
482 doi:10.1016/j.jhydrol.2017.02.020

483 Wu, Z. I., Ma, B. Y., Wang, H. L., Hu, C. H., Lv, H., & Zhang, X. Y. (2021).  
484 Identification of Sensitive Parameters of Urban Flood Model Based on  
485 Artificial Neural Network. *Water Resources Management*, 35(7), 2115-2128.  
486 Retrieved from <Go to ISI>://WOS:000646644200001.  
487 doi:10.1007/s11269-021-02825-3

488 Wu, Z. N., Ma, B. Y., Wang, H. L., & Hu, C. H. (2020). Study on the Improved  
489 Method of Urban Subcatchments Division Based on Aspect and Slope- Taking  
490 SWMM Model as Example. *Hydrology*, 7(2), 17. Retrieved from <Go to



491 ISI>://WOS:000551260500009. doi:10.3390/hydrology7020026

492 Xiang, C., Liu, J., Wang, H., & Shao, W. (2017). Monitoring and Simulation of Urban  
493 Hydrological Unit: A Case Study of Tsinghua University, Beijing. [城市水文  
494 单元雨洪监测与模拟研究-以清华大学校园为例]. *Journal of China  
495 Hydrology*, 37(4), 12-17. Retrieved from <Go to ISI>://CSCD:6058698.

496 Xu, H. S., Ma, C., Xu, K., Lian, J. J., & Long, Y. (2020). Staged optimization of urban  
497 drainage systems considering climate change and hydrological model  
498 uncertainty. *Journal of Hydrology*, 587, 11. Retrieved from <Go to  
499 ISI>://WOS:000568819100081. doi:10.1016/j.jhydrol.2020.124959

500 Zaghoul, N. A. (1983). SENSITIVITY ANALYSIS OF THE SWMM  
501 RUNOFF-TRANSPORT PARAMETERS AND THE EFFECTS OF  
502 CATCHMENT DISCRETIZATION. *Advances in Water Resources*, 6(4),  
503 214-223. Retrieved from <Go to ISI>://WOS:A1983SS39100004.  
504 doi:10.1016/0309-1708(83)90059-3

505 Zhang, N., Li, N., Gan, H., & Wang, J. (2017). Improvement of underground drainage  
506 computation method for urban flood simulation model. *Journal of Hydraulic  
507 Engineering*, 48(5), 526-534. Retrieved from <Go to ISI>://CSCD:6001685.

508 Du Xian. (2020). Research on refined simulation of urban rainstorm and flood based  
509 on SWMM model. (Master), Zhengzhou University, Available from Cnki

510 Fu Xiaoran, Wang Dong, Luan Qinghua, Liu Jiahong, & Wang Haichao. (2020).  
511 Construction and simulation of large-scale pipeless flow data urban  
512 SWMM——II. Model parameter verification and storm runoff simulation

513 analysis. *Advances in Water Science*, 31 (01), 51-60.

514 Liu Kexin, Bao Weimin, Que Jiajun, Li Jiajia, & Shu Huilian. (2015). Application of  
515 K-means clustering method based on principal component analysis in flood  
516 forecasting. *Journal of Wuhan University (Engineering Edition)*, 48(04), 447  
517 -450+458.

518 Liu Xingpo. (2009). Urban rainfall runoff model parameter calibration method based  
519 on runoff coefficient. *Water Supply and Drainage*, 45(11), 213-217.

520 Luan Qinghua, Fu Xiaoran, Wang Haichao, Liu Jiahong, & Gao Xuerui. (2019).  
521 Construction and simulation of SWMM for large-scale urban area without  
522 pipe flow data—I. Key technology for digital refinement of complex  
523 underlying urban area. *Advances in Water Science*, 30 (05), 653-660.

524 Mei Chao. (2019). Urban hydrology and hydrodynamic coupling model and its  
525 application research. (Ph.D.), China Institute of Water Resources and  
526 Hydropower Research, Available from Cnki

527 Mei Chao, Liu Jiahong, Wang Hao, Li Zejin, Xia Lin, & Wang Ying. (2017). SWMM  
528 principle analysis and application prospects. *Water Resources and  
529 Hydropower Technology*, 48(05), 33-42.

530 Qian Kun, Bao Weimin, Li Sisong, & Si Wei. (2012). Application of K-means cluster  
531 analysis method in flood forecasting. *Hydropower Energy Science*, 30(05),  
532 41-44.

533 Xu Yuanhao, Wu Qiang, Li Changqing, Chen Youqian, Zhang Li, Ran Guang, & Hu  
534 Caihong. (2020). Simulation and prediction of flood process in the middle  
535 reaches of the Yellow River based on long short-term memory (LSTM) neural  
536 network. *Journal of Beijing Normal University (Natural Science Edition)*,  
537 56(03), 387-393.

# Figures

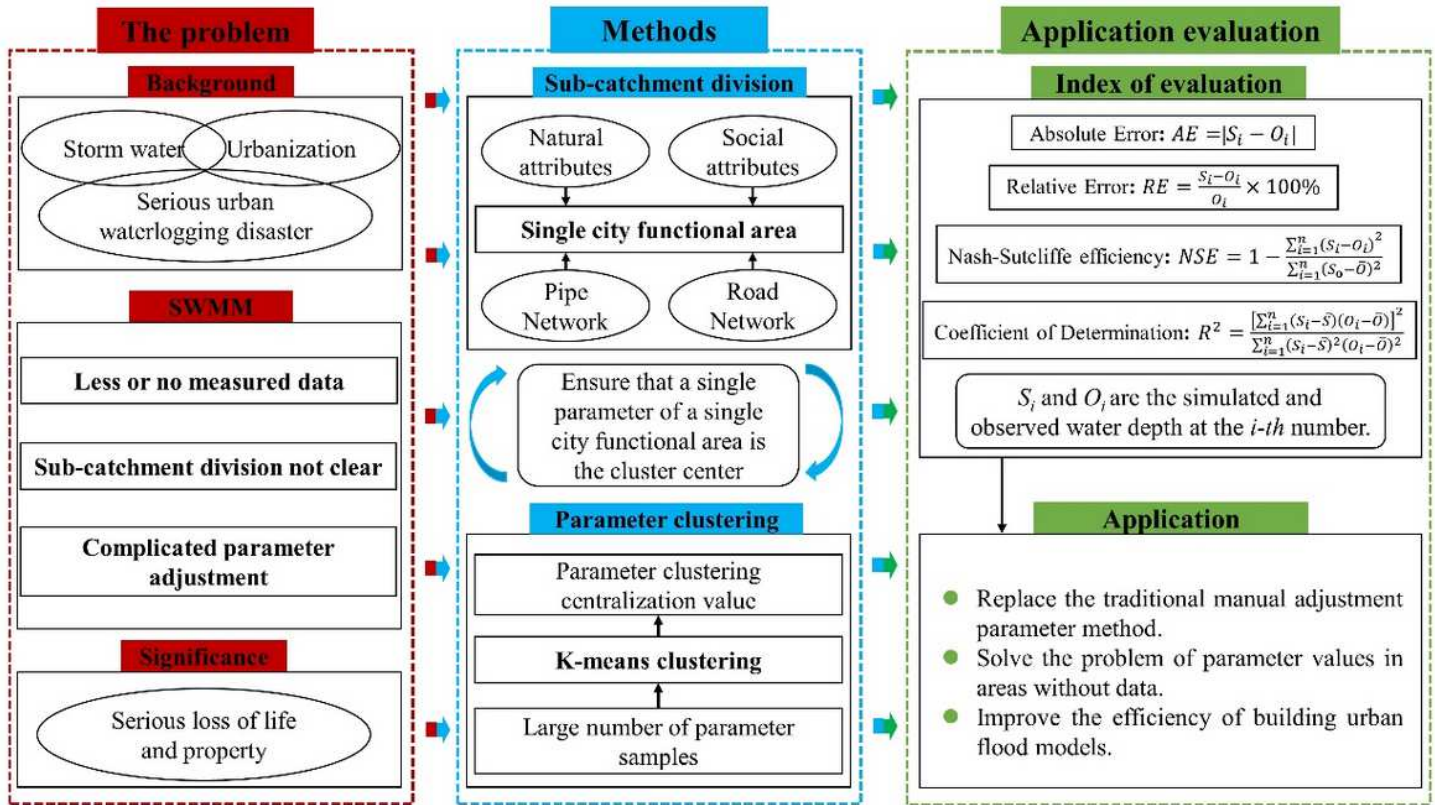


Figure 1

Research frame diagram.



Figure 2

Study area.

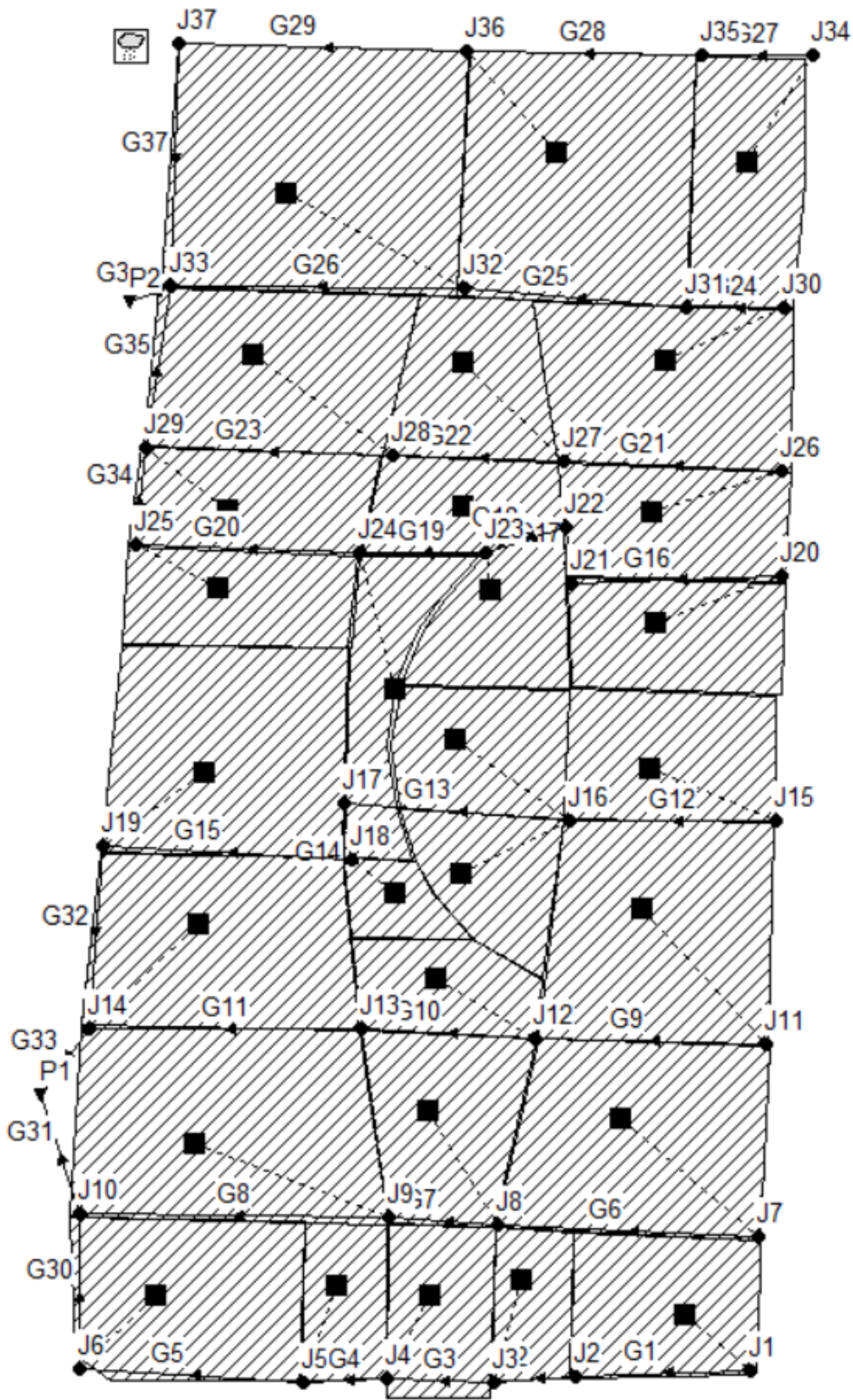
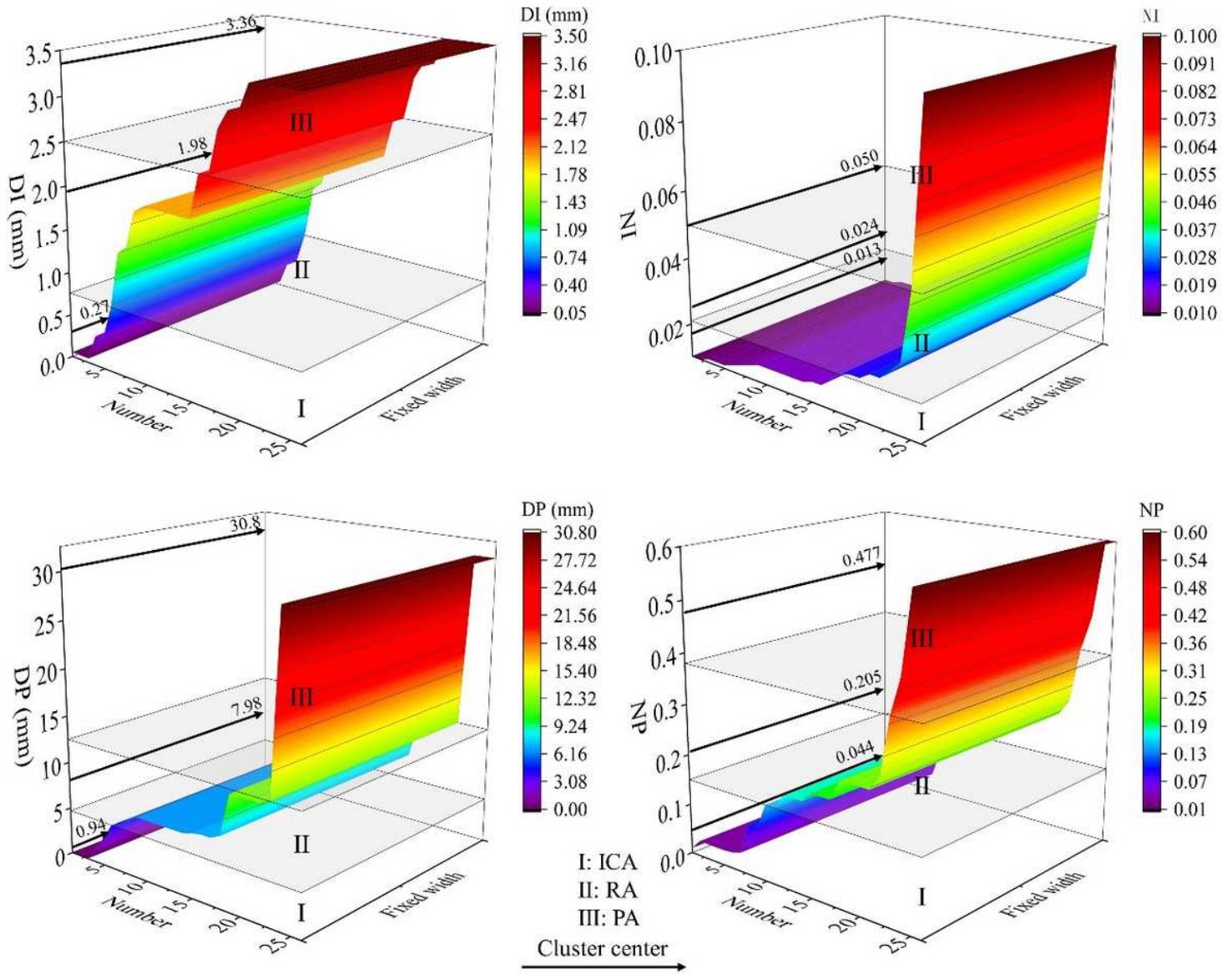


Figure 3

Generalized map of the sub-catchment in the study area.



**Figure 4**

Parameter clustering results.

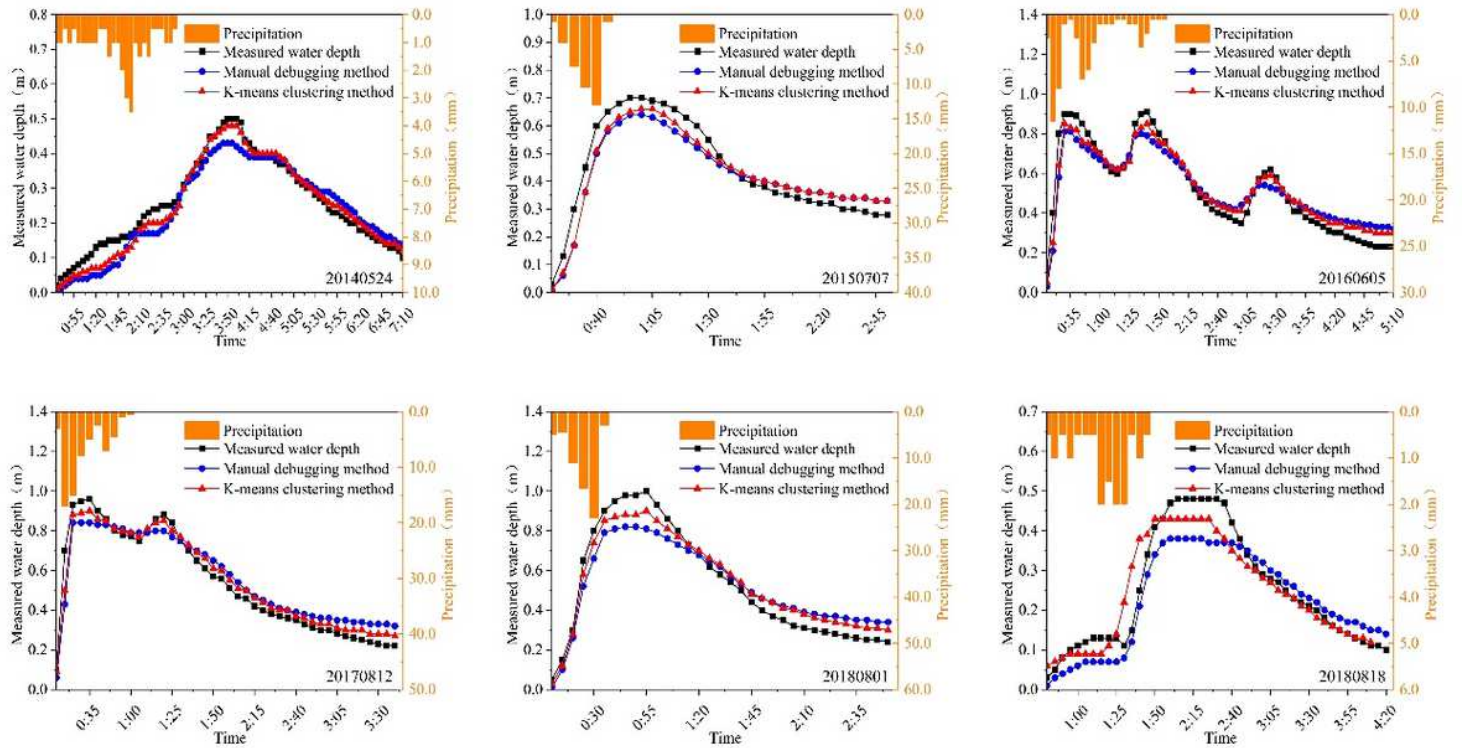


**Figure 5**

Observed and estimated hydro-graphs of the Manual debugging method and K-means clustering method in SWMM model at the validation stage in 6 flood events.

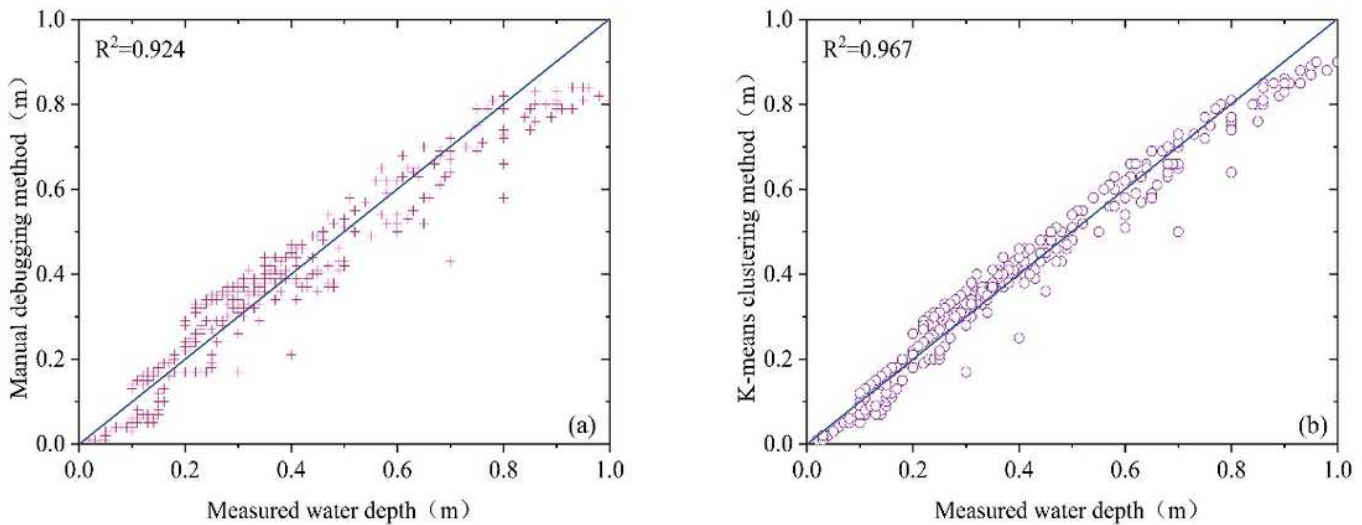


**Figure 6**

Correlation coefficient graph.